

Charge dynamics of a molecular ion immersed in a Rydberg-dressed atomic lattice gas

Rick Mukherjee^{1,2}

¹*Department of Physics, Indian Institute of Science Education and Research, Bhopal, India*

²*Department of Physics, Imperial College, SW7 2AZ, London, UK*

(Dated: June 20, 2022)

Charge dynamics in an ultra-cold setup involving a laser dressed atom and an ion is studied here. This transfer of charge is enabled through molecular Rydberg states that are accessed via a laser. The character of the charge exchange crucially depends on the coupling between the electronic dynamics and the vibrational motion of the atoms and ion. The molecular Rydberg states are characterized and a criterion for distinguishing coherent and incoherent regimes is formulated. Furthermore the concept is generalized to the many-body setup as the ion effectively propagates through a chain of atoms. Aspects of the transport such as its direction can be controlled by the excitation laser. This leads to new directions in the investigation of hybrid atom-ion systems that can be experimentally explored using optically trapped strontium atoms.

Ultracold atoms in optical lattices opened the door for experimental studies of a wide range of quantum many-body problems [1, 2]. Similar breakthroughs have been achieved in trapped ion systems [3–11]. Emerging from these efforts is a growing interest in exploring hybrid systems formed of trapped atoms and ions [12–17]. This combination enables access to a plethora of novel phenomena such as strongly coupled polaron states [18–20], long-range collisions [21–23], electron-phonon coupling in Fermi gases [24], the study of many-body quantum dynamics and correlations [25–27], atom-ion quantum gates [28], quantum switches for information transfer [29, 30] as well as the formation of mesoscopic molecular ions [31, 32].

Charge exchange are processes central in atom-ion systems and has relevance in the study of chemical reactions [22, 33] as well as charge transport in the ultra-cold domain [34]. Resonant charge exchange in atom-ion setups plays a crucial role in the cooling of ions [35, 36]. At sufficiently low temperatures, the mechanism for charge exchange involves electron hopping from neutral atoms to a neighbouring ion. However, for ground state atoms, the probability for such a hopping process to occur is highly suppressed due to the negligible overlap between the electron wave function with the orbital of a nearby ion. This unfavourable situation can change for highly excited (Rydberg-)atoms [37] where the large spatial extent of the electronic wave function enhances the probability for electron hopping onto the ion [38].

The aim of this work is to investigate the charge dynamics in an atom-ion hybrid system that is formed by a deep optical lattice filled with a single atom per site out of which one is ionized. Before moving to the many-body problem, we first study the two body problem involving the atom and an ion. The underlying key ingredient is the existence of electronic molecular Rydberg states that encompass the ion and an adjacent atom. The electronic wave function of the ground state atom has a negligible overlap with the neighbouring ion. But for a Rydberg atom, the wave function of the electron has a large spatial

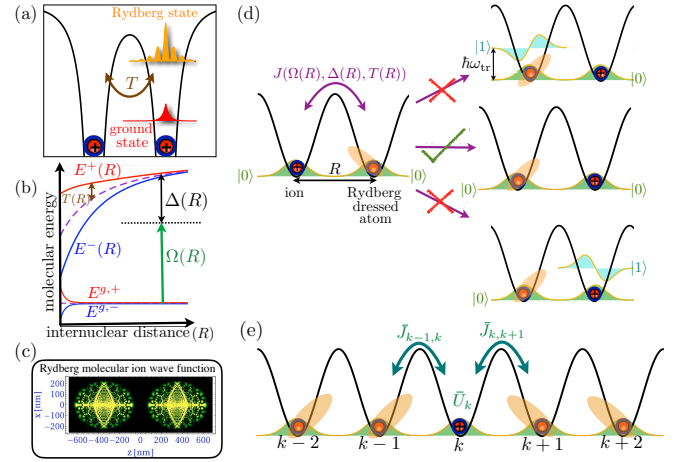


FIG. 1. (a) Illustration of the key principle: While a low-lying state (shown in red) can remain localized, a Rydberg state (shown in orange) can tunnel through the ionic potential barrier (black lines) at a rate T . (b) A laser addresses the excited Rydberg molecular states with effective coupling $\Omega(R)$ and detuning $\Delta(R)$ that depend on the intra-molecular separation. Tunneling ($T(R)$) is given by the splitting between the gerade ($E^+(R)$) and ungerade ($E^-(R)$) states which are in fact the electronic molecular ion states. (c) Depicting the probability density for a specific molecular ion state. (d) In the Rydberg dressed picture, J is the effective hopping term of the electron between the dressed ground state atom and ion. Coherent dynamics is facilitated by confining the ion and the Rydberg dressed atom in an identical double well optical trap. Initially prepared in their motional ground states $|0\rangle$ (shown in green), the coupling to higher motional states such as $|1\rangle$ (shown in aquamarine) are suppressed by choosing optimum optical and trapping conditions. (e) The two particle picture can be generalized to obtain the effective many-body charge transport model with nearest neighbour hopping $J_{k,k\pm 1}$ and on-site energy \bar{U}_k (refer to text).

extension which enhances the hopping probability as depicted in Fig. 1(a). The tunneling rate is determined by the splitting between the corresponding potential curves of opposite symmetry as shown in Fig. 1(b). However, en-

hanced tunneling occurs at inter-nuclear distances where the Rydberg atom is considerably polarised by the ion leading to strong l-mixing of the Rydberg states resulting in the formation of complex Rydberg molecular ion states as shown in Fig. 1(c). Thus in the presence of a detuned laser, the ground state atom couples to more than one Rydberg state described by a dressed atom picture. In this picture, the focus is on dressed states whose major contribution is from the ground state with a small fraction of Rydberg molecular ion states. These states have long lifetimes. The effective hopping rates J for these long-lived dressed states are derived, which implicitly depend on the inter-nuclear distance via the electronic tunneling $T(R)$ as well as the optical parameters $(\Delta(R), \Omega(R))$ as depicted in Fig. 1(b). The strong dependence of the effective charge hopping rate on inter-atomic distance leads to the coupling between electronic and vibrational dynamics which may effectively cause decoherence in the charge transfer. This coupling between electronic and vibrational degrees of freedom can be minimised by trapping the atoms and the ion in an identical potential [see Fig. 1(d)] which can be achieved with strontium [39]. The natural extension of the two particle picture to the many-body system leads to de-localised charge dynamics which is interesting in its own right. However, in certain regimes of the parameter space, it is shown that the many-body charge dynamics is effectively dictated with nearest neighbour hopping as shown schematically in Fig. 1(e).

RYDBERG MOLECULAR ION

The Rydberg molecular ion states are calculated for strontium (Sr) by adopting a linear combination of localized orbitals. The orbitals (ψ_{nl}) correspond to Rydberg states of Sr obtained using a single active electron approximation [42]. The electronic Hamiltonian in atomic units for the two particle case consisting of an ion adjacent to a Rydberg atom is given as

$$H_{\text{el}}(r_1, r, R) = -\frac{\nabla_r^2}{2} - \frac{1}{r_1} - \frac{1}{r_2} + \frac{1}{R}, \quad (1)$$

where r is the position of the Rydberg electron, $r_{i=1,2}$ are the relative position of the Rydberg electron with respect to either nucleus and R is the inter-nuclear distance between the nuclei. Owing to the non-orthogonality between the Rydberg wave functions (ψ_{nl}) defined at either nuclei, there is a small but non-zero overlap function. However for this work, the focus is on inter-nuclear distances where these overlap integrals are small thereby obtaining a simplified eigenvalue problem for the above Hamiltonian. Upon diagonalization, we have the Rydberg molecular states, $|ie^\alpha\rangle$ or $|e^\alpha i\rangle$ depending on whether the Rydberg atom is to the right or left

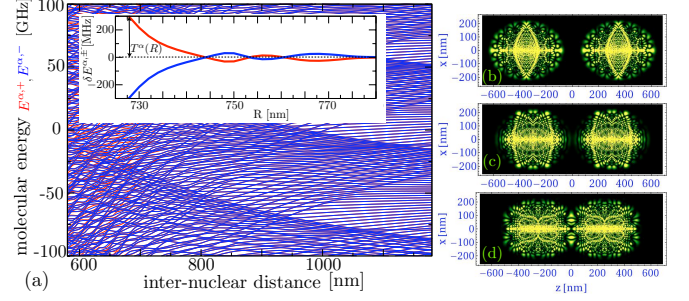


FIG. 2. (a) Potential curves for high lying Rydberg states of a Sr_2^+ molecular ion. The molecular energies are given relative to the $\text{Sr}_2^+(50S)$ asymptote. The relative energies, $\delta E^{\alpha,(\pm)} = E^{\alpha,(\pm)} - (E^{\alpha,+} + E^{\alpha,-})/2$, of a selected pair (thick lines) with (un)gerade symmetry is shown in the inset for which the tunnel splitting is as large as several 100 MHz at an internuclear distance of $R = 730$ nm. (b-d) Plotting the complex Rydberg molecular ion wave functions for selected pair of potentials shown in the inset for three different inter-nuclear distances, 700 nm in (b), 670 nm in (c) and 640 nm in (d).

of the ion. The interactions of the Rydberg molecular ion is invariant with respect to exchange in nuclear positions and it is always possible and often convenient to express the molecular states in the (un)gerade basis, $|e^{\alpha,(\pm)}\rangle = 1/\sqrt{2}(|ie^\alpha\rangle \pm |e^\alpha i\rangle)$ and their corresponding energies $E^{\alpha,(\pm)}(R)$. The index $\alpha = 1, 2, \dots$ represents the different excited states of the Rydberg molecular ion. Compared to calculations of low-lying states, those for highly excited molecules prove very demanding due to the need for a large basis set and the highly oscillatory character of the involved atomic Rydberg states. Fig. 2(a) depicts a characteristic pair of molecular potential curves $E^{\alpha,(\pm)}(R)$ around the $\text{Sr}^+(50S)$ asymptote, obtained for a basis set of $\sim 10^3$ atomic states. At such high excitations, the ion-atom interaction leads to strong state mixing already at micrometer distances which is reflected in the molecular ion wave functions shown in Fig. 2(b)-(d). The charge exchange between the ion and Rydberg atom is determined by the energy splitting given as

$$T^\alpha(R) = \frac{E^{\alpha,+}(R) - E^{\alpha,-}(R)}{2}. \quad (2)$$

There is substantial tunnel splitting between the opposite symmetry states [see inset of Fig. 2] of up to several hundred MHz, even at distances for which the Rydberg electron remains well localized at either ionic core.

OPTICAL COUPLING TO RYDBERG MOLECULAR ION STATES

Using the two particle notation introduced in the previous section, the ion and the ground state atom of Sr is denoted by $|ig\rangle$ or $|gi\rangle$ depending on the position of

the respective particles, where $|g\rangle = |5s^2, ^1S_0\rangle$. The optical coupling of $|ig\rangle, |gi\rangle$ to $|ie^\alpha\rangle, |e^\alpha i\rangle$ respectively is a two photon process via the inter-mediate triplet state, $5s5p, ^3P_1$ with an effective Rabi frequency $\Omega^\alpha(R)$. The coupling is determined by the dipole matrix element, $\mu^\alpha(R) = \langle 5s5p | \mu | e^\alpha(R) \rangle$. The natural decay rate for the low lying intermediate state $5s5p, ^3P_1$ is $21 \mu\text{s}$. By increasing the detuning with respect to the inter-mediate state, the lifetime is increased to 8.4 ms . This requires that the effective Rabi frequency for the two photon excitation scheme is of the order of tens of MHz, which remains experimentally achievable [46–48]. In order to relate this coupling strength to that of neutral gas experiments, all Rabi frequencies are expressed in terms of a reference Rabi frequency, Ω_{5s}^{50s} , for an isolated atom which for our purposes is chosen to be 40 MHz . Detuning of the laser with respect to a particular molecular Rydberg state is given as $\Delta^\alpha(R) = \omega_L - (E^{\alpha,-}(R) + E^{\alpha,+}(R))/2$ where ω_L is the frequency of the second photon. Using the dipole approximation for the laser field and the rotating wave approximation, the resulting Hamiltonian is

$$\hat{H}_{\text{opt}}^{\text{tp}}(R) = \sum_{\alpha} \left[-\Delta^\alpha(R) (|ie^\alpha\rangle\langle ie^\alpha| + |e^\alpha i\rangle\langle e^\alpha i|) \right. \\ \left. + \frac{\Omega^\alpha(R)}{2} (|ig\rangle\langle ie^\alpha| + |gi\rangle\langle e^\alpha i| + \text{h.c.}) \right. \\ \left. + T^\alpha(R) (|ie^\alpha\rangle\langle e^\alpha i| + \text{h.c.}) \right]. \quad (3)$$

The electronic ground states energies are set to zero. The Hamiltonian $\hat{H}_{\text{opt}}^{\text{tp}}$ is diagonalized to obtain exact solutions for the laser-dressed molecular states, $|d_\beta\rangle$ along with the energies $\omega^\beta(R)$ (\hbar is set to 1). $|d_\beta\rangle$ are expressed in terms of a superposition of the electronic ground states $|ig\rangle, |gi\rangle$ as well as the molecular excited states $|ie^\alpha\rangle, |e^\alpha i\rangle$. The index $\beta = 1, 2, \dots$ represents the different dressed states. Of major interest is the pair of molecular states that has the largest contribution of electronic ground states. These states correspond to states with large lifetimes and are denoted by $|\tilde{g}_{1,2}\rangle$ with energies $\omega_{1,2}^{\tilde{g}}(R)$. Expressing the electronic dynamics as effective hopping between the relevant dressed states, we have

$$\hat{H}_{\text{effec}}^{\text{tp}}(R) = U(R) (|\tilde{g}\rangle\langle\tilde{g}| + |\tilde{g}i\rangle\langle\tilde{g}i|) \\ + J(R) (|\tilde{g}\rangle\langle\tilde{g}i| + \text{h.c.}) . \quad (4)$$

where $U(R) = \langle\tilde{g}|\hat{H}_{\text{effec}}^{\text{tp}}(R)|\tilde{g}\rangle = \langle\tilde{g}i|\hat{H}_{\text{effec}}^{\text{tp}}(R)|\tilde{g}i\rangle$ is the light shift associated with ion-dressed atom pair and $J(R) = \langle\tilde{g}|\hat{H}_{\text{effec}}^{\text{tp}}|\tilde{g}i\rangle$ is the effective hopping. In this simple two particle picture, the details of the Rydberg state and its admixture to the relevant dressed atom is determined by the laser parameters which is included in the definitions of $U(R)$ and $J(R)$.

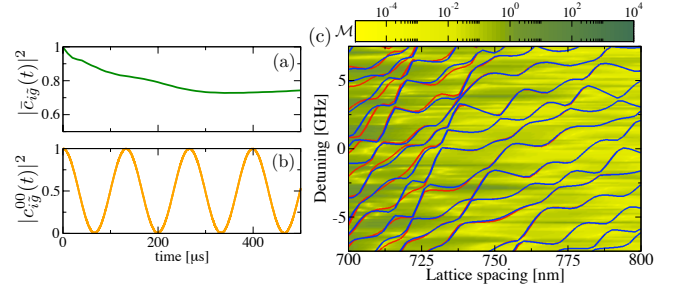


FIG. 3. (a) Effective classical ion dynamics shown for an untrapped ion-atom pair by plotting $|\bar{c}_{ig}(t)|^2$ which is calculated by averaging $c_{ig}(R, t)$ obtained from Eq. (5) over the inter-nuclear distance. (b) The plot shows the probability for the ion to be at a given site in its motional ground state for a double well with trapping frequency $\omega_{tr} = 500 \text{ kHz}$. (c) For the same trapping frequency as (b), a colour density plot is shown for \mathcal{M} (see Eq. (7)) distinguishing coherent dynamics ($\mathcal{M} \ll 1$) from incoherent dynamics ($\mathcal{M} \geq 1$) for a range of detunings and lattice spacings. For example, the detuning for dynamics shown in (b) is -0.7 GHz with lattice spacing 796 nm corresponding to $\mathcal{M} = 0.044$.

CHARGE DYNAMICS WITH CLASSICAL AND QUANTUM MOTION OF RYDBERG-DRESSED MOLECULAR ION

Here classical motion refers to an unconfined pair of Rydberg dressed ground state atom and ion in which electron transfer occurs. The instantaneous state for classical dynamics is given by $|\psi(R, t)\rangle = c_{ig}(R, t)|i\tilde{g}\rangle + c_{gi}(R, t)|\tilde{g}i\rangle$ and the corresponding equations of motion using Eq. (4) are

$$i\partial_t c_{ig}(R, t) = U(R)c_{ig}(t) + J(R)c_{gi}(t), \quad (5)$$

$$i\partial_t c_{gi}(R, t) = U(R)c_{gi}(t) + J(R)c_{ig}(t). \quad (6)$$

For a fixed inter-nuclear distance R , one obtains the probability to be in state $|i\tilde{g}\rangle$ or $|\tilde{g}i\rangle$ to be $\cos^2[J(R)t]$. However for a free pair of particles, one obtains different hopping rates corresponding to different inter-nuclear distances. On averaging over the inter-nuclear distance, the probability to obtain a particular two particle state, for example $|i\tilde{g}\rangle$ is given by $|\bar{c}_{ig}(R, t)|^2$ and is shown to slowly decay as seen in Fig.3(a). In order to control the uncertainty in the position of either particle (ion/atom) and thereby get a better handle on the coherence of the dynamics, we propose to have an identical confinement for the ion and atom, which is achievable for alkaline-earth atoms [39]. This would correspond to the quantum motion of the Rydberg dressed ground state atom and ion (as depicted in Fig. 1(d)). In a double well, the electronic and motional degrees of freedom are entangled in the overall state given as $|\psi\rangle = \sum_{n,n'} (c_{ig}^{n,n'}(t)|i\tilde{g}\rangle|nn'\rangle + c_{gi}^{n,n'}(t)|\tilde{g}i\rangle|nn'\rangle)$. Here $|nn'\rangle$ is the eigenstate of the Hamiltonian corresponding to the center of mass dynamics for two particles in a dou-

ble well harmonic trap [40]. For typical trapping frequencies of few hundred kHz, the nuclear dynamics within the trap is much slower than the electronic dynamics and is solved under the Born-Oppenheimer approximation. It is assumed that the system is prepared in the lowest motional state denoted by $|00\rangle$. The probability to excite the first motional state can be calculated from the off-diagonal couplings $\langle 00|U(R)|01\rangle$ and $\langle 00|J(R)|01\rangle$. As long as the off-diagonal couplings are smaller than the trapping frequency ω_{tr} and the corresponding light shifts, we have coherent dynamics. To quantify the degree to which we couple the lowest motional states to their next higher motional state, the following parameter is introduced,

$$\mathcal{M} = \frac{|U_{00}^{01} + J_{00}^{01}|}{|U_{01}^{01} - U_{00}^{00} + \omega_{\text{tr}}|}, \quad (7)$$

where $A_{n'm'}^{nm} = \langle nm|A(R)|n'm'\rangle$ and $A \in \{U, J\}$. If the coupling of $|00\rangle$ to $|01\rangle$ is small enough then the coupling to higher motional states such as $|02\rangle$ (or $|20\rangle$) are suppressed as well since they are higher order processes. Thus, the lower the value of \mathcal{M} , the more coherence is expected in the charge dynamics. As is expected, for sufficiently large trapping frequencies, it is possible to suppress the population of higher motional states. However there are experimental limitations to how large the optical trap frequency can be and the typical values of $(U_{01}^{01} - U_{00}^{00})$ are comparable to ω_{tr} . Thus to have lower values of \mathcal{M} , we need $|U_{00}^{01}|, |J_{00}^{01}| \ll |U_{01}^{01} - U_{00}^{00}|$, which is easily satisfied for large enough lattice spacings. In Fig. 3(c), \mathcal{M} is represented in a two dimensional colour plot for different values of detuning and lattice spacing for a fixed trapping frequency of $\omega_{\text{tr}} = 500$ kHz. It is always possible to find suitable lattice spacing and detuning to obtain coherent dynamics for our chosen trap frequency. Whenever we work in the regime where the higher motional states are not populated, we can replace $U(R)$ and $J(R)$ by $\bar{U} = U_{00}^{00}$ and $\bar{J} = J_{00}^{00}$ respectively.

GENERALIZATION TO MANY-BODY CHARGE TRANSPORT

In this section, the two particle picture will be generalized to many particles where we have a deep optical lattice filled with a single atom per site out of which one is ionized. In the many-particle system, we assume lattice spacings such that the actual tunneling $T(R)$ of the Rydberg electron is dominant for atoms that are nearest neighbours to the ion. For now we focus on the optical coupling of the many-body system and include the motional states in next section, where we work in the coherent regime. To this effect, we have the following reduced basis for the many-particle picture: all atoms in the ground state with an ion at site k ($|I_k\rangle = |g_1 \dots g_{k-1} \ i_k \ g_{k+1} \dots g_N\rangle$), a Rydberg atom to

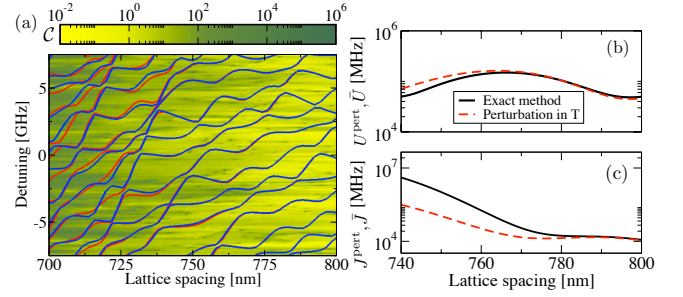


FIG. 4. (a) Density plot shows the relative difference in the dynamical parameters defined in \mathcal{C} (see Eq. (10)). \mathcal{C} is calculated using exact as well as perturbative methods (refer to text) for different laser parameters. The light regions in the density plot correspond to parameter space where the perturbation method agrees with the exact method. (b)-(c) U and J averaged over motional ground states is shown for a particular detuning, $\Delta = -0.7$ GHz.

the right of the ion ($|R_k^\alpha\rangle = |g_1 \dots g_{k-1} \ i_k \ e_{k+1}^\alpha \dots g_N\rangle$) and a Rydberg atom to the left of the ion ($|L_k^\alpha\rangle = |g_1 \dots e_{k-1}^\alpha \ i_k \ g_{k+1} \dots g_N\rangle$). The Hamiltonian for the optical coupling of the many-body system is given as

$$\begin{aligned} \hat{H}_{\text{opt}}^{\text{mp}} = & \sum_{\alpha} \sum_{k=1}^N \left[-\Delta_k |R_k^\alpha\rangle \langle R_k^\alpha| + \frac{\Omega_k}{2} (|R_k^\alpha\rangle \langle I_k| + \text{h.c.}) \right. \\ & \left. -\Delta_k |L_k^\alpha\rangle \langle L_k^\alpha| + \frac{\Omega_k}{2} (|L_k^\alpha\rangle \langle I_k| + \text{h.c.}) \right] \\ & + \sum_{\alpha} \sum_{k=1}^{N-1} \frac{T_k}{2} [|R_k^\alpha\rangle \langle L_{k+1}^\alpha| + \text{h.c.}] . \end{aligned} \quad (8)$$

On comparing with Eq. (3), we find that the dependence of the optical parameters and the tunneling on distance R has been replaced by subscript k , which denotes the site number of the ion placed within the atomic lattice. Similar to the two particle picture, we can diagonalize $\hat{H}_{\text{opt}}^{\text{mp}}$ to obtain dressed states and focus on the many-body Rydberg-dressed ground states denoted as $|\tilde{I}^k\rangle = |\tilde{g}_1 \dots \tilde{g}_{k-1} \ i_k \ \tilde{g}_{k+1} \dots \tilde{g}_N\rangle$. Typically in the two particle picture, the excitation laser couples the ground state atom to its Rydberg states, the electron tunnels to its neighboring ion and the newly positioned excited atom couples back to its ground state. However, in the many-particle picture, the electron can in principle tunnel multiple times across the lattice before it couples back to the ground state atom. Thus although we assume nearest neighbour tunneling and work in the reduced basis, we find that the effective ion dynamics in the Rydberg-dressed atom filled optical lattice is delocalised. This implies that the effective equations of motion couple $|\tilde{I}_k\rangle$ not only to $|\tilde{I}_{k\pm 1}\rangle$ but also to $|\tilde{I}_{k\pm 2}\rangle$ and so on. Unlike in the two particle picture, where we obtain an effective Hamiltonian for charge transfer (see Eq. (4)) with $J(R)$ as the exchange term between the neighbouring Rydberg dressed ground state atom and the ion, the effective dy-

namics in the many-body setup cannot be described simply by its nearest neighbour exchange term unless we include additional constraints. However, using time independent perturbation theory where $T_k \ll \Omega_k$ for all k , it is possible to derive the nearest neighbour hopping term. The effective Hamiltonian obtained in this limit describes charge dynamics for an ion in Rydberg dressed atomic lattice,

$$\begin{aligned} \hat{H}_{\text{effec}}^{\text{mp}} = & \sum_k U_k \left(|\tilde{I}_k\rangle\langle\tilde{I}_k| \right) \\ & + J_{k,k+1} \left(|\tilde{I}_{k+1}\rangle\langle\tilde{I}_k| + \text{h.c.} \right) \\ & + J_{k,k-1} \left(|\tilde{I}_{k-1}\rangle\langle\tilde{I}_k| + \text{h.c.} \right), \end{aligned} \quad (9)$$

where $U_k = \langle\tilde{I}_k|\hat{H}_{\text{effec}}^{\text{mp}}|\tilde{I}_k\rangle$ and $J_{k,k+1} = \langle\tilde{I}_k|\hat{H}_{\text{effec}}^{\text{mp}}|\tilde{I}_{k+1}\rangle$. To identify regimes in the parameter space where the perturbation theory is valid we resort back to the two particle picture. We derive dynamical parameters ($U^{\text{pert}}, J^{\text{pert}}$) by solving $\hat{H}_{\text{opt}}^{\text{tp}}$ perturbatively in the limit $\Omega \gg T$. Averaging over the motional states, $U^{\text{pert}}, J^{\text{pert}}$ are compared to \bar{U}, \bar{J} which were obtained by solving Eq. (4) without any approximation (referred to as exact method in Fig. 4(b)-(c)). This is numerically quantified by the following parameter,

$$\mathcal{C} = \left| \frac{\bar{U} - U^{\text{pert}}}{\bar{U}} \right| + \left| \frac{\bar{J} - J^{\text{pert}}}{\bar{J}} \right|. \quad (10)$$

Fig. 4(a) shows the different values of \mathcal{C} for different laser parameters and lattice spacing. As expected, for larger lattice spacings, the overall T is smaller which easily satisfies our condition for perturbation theory and corresponds to lower values of \mathcal{C} . This is further confirmed in Fig. 4(b)-(c) where we compare the dynamical parameters from two different methods.

COHERENT MANY-BODY CHARGE TRANSPORT WITH NEAREST-NEIGHBOUR HOPPING

The theory for charge transport over many-sites can be understood using the simple model of pair-wise charge exchange at two sites involving the ion and its neighbouring atom. Having identified the optimum optical parameters and lattice spacing in prior sections to have nearest neighbour coherent hopping, we use them in our numerical simulation for charge dynamics involving a single ion and $N - 1$ atoms in a one dimensional optical lattice. The optimum lattice spacings is around 750-850 nm for Sr atoms excited off-resonantly to 50s Rydberg state with negative detunings 0.7 – 1 GHz giving overall dynamical timescales in the order of tens to hundreds of μs . This is much lower than the decay time of the intermediate state (8.4 ms) to which we couple off-resonantly

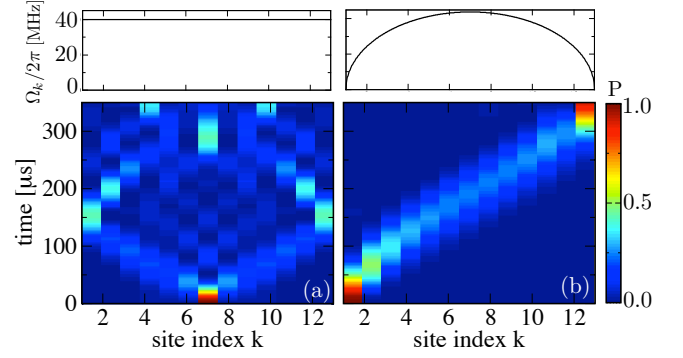


FIG. 5. Density plot shows the probability of the ion during its dynamics in a Rydberg dressed lattice with a specific lattice spacing of 796 nm and laser detuning -0.7 GHz with the top panels showing the corresponding Rabi profile of the excitation laser: (a) Constant Rabi frequency, $\Omega_c = 40$ MHz, where $J_0 = \bar{J}_{k,k+1} = 27$ kHz and $U_0 = \bar{U}_k = 15.9$ kHz for all values of k . (b) Varying Rabi profile along the x-direction, $\Omega_k(x) = \Omega_c \sqrt{(N-kx)(k-1)x}$ such that $\bar{J}_{k,k+1} = (2J_0/N) \sqrt{(N-k)k}$ and $\bar{U}_{k,k+1} = (2U_0/N) \sqrt{(N-k)k}$.

as well as the typical spontaneous decay of the Rydberg states which is estimated to be 250-350 ms using [45]. We ignore the accidental resonances to Rydberg states or doubly excited states since the probability for it to occur is small ($\sim 10^{-2}$) particularly when averaged over the motional states. Solving for $\Psi = \sum_{k=1}^N \tilde{C}_k^I |\tilde{I}_k\rangle$ using the many-body Hamiltonian Eq. (9) gives

$$i\partial_t \tilde{C}_k^I = \bar{U}_k \tilde{C}_k^I + \bar{J}_{k,k-1} \tilde{C}_{k-1}^I + \bar{J}_{k,k+1} \tilde{C}_{k+1}^I, \quad (11)$$

where $\bar{U}_k = \langle 00|U_k|00\rangle$ and $\bar{J}_{k,k+1} = \langle 00|J_{k,k+1}|00\rangle$. In general, $\bar{J}_{k,k+1}$ does not have to be equal to $\bar{J}_{k+1,k}$. Fig. 5 depicts the results of the numerical simulation for 13 sites with different laser profiles. Focusing on the excitation laser with constant Rabi profile [see Fig. 5(a)], we have an ion initially located at site 7 which then propagates in both directions symmetrically as it has equal probability to hop in either direction at every instant. A scenario involving spatially varying Rabi profile is depicted in Fig. 5(b). In this case $\bar{J}_{k,k+1} \neq \bar{J}_{k+1,k}$ and the Rabi profile has been chosen in such a manner that it mimics motion of a particle in harmonic well [44] with its minima at the center (site 7 in this case). Hence an ion situated at site 1 is akin to starting at one end of the well which then propagates through site 7 with maximum kinetic energy till it reaches the other end. The role of the light shift \bar{U}_k is simply an additional energy shift experienced by the atoms/ion in the lattice. This can be compensated by choosing an appropriate profile for the trapping laser.

CONCLUSION

In this work, we propose and model the effective charge dynamics of an ion within trapped Sr atoms in an optical lattice. We conclude that optically trapped alkaline-earth atoms-ion systems can naturally serve as a platform for the study of charge transfer in a controlled many-body environment. Control of the coherence in the charge dynamics requires the dressing of ground state atoms to their Rydberg states [49, 50] and the provision of identical confinement for both the ion and the Rydberg-dressed atom [39], both of which are potentially attainable with ongoing experiments with alkaline-earth atoms [51–55]. Finally, such systems are promising for the quantum simulation of novel ultra-cold chemistry [56], exciton transport [57] and Fröhling type Hamiltonians that occur in condensed matter systems [24].

R.M would like to acknowledge I. Lesanovsky and T. Pohl for their invaluable input and discussion. R.M would also like to acknowledge S. Wüster for his discussion and the Max-Planck society for funding under the MPG- IISER partner group program.

-
- [1] I. Bloch Nat. Phys. 1, 23 (2005).
 - [2] M. Greiner, O. Mandel, T. Esslinger, T. W. Hänsch and I. Bloch Nature 415, 39 (2002).
 - [3] J. I. Cirac and P. Zoller Phys. Rev. Lett. 74, 4091 (1995).
 - [4] P. Schindler, D. Nigg, T. Monz, J. T. Barreiro, E. Martinez, S. X. Wang, S. Quint, M. F. Brandl, V. Nebendahl and C. F. Roos J. Phys. 15 123012 (2013).
 - [5] B. B. Blinov, D. L. Moehring, L.M. Duan and C. Monroe Nature 428, 153 (2004).
 - [6] R. Blatt and C. F. Roos Nat. Phys. 8, 277 (2012).
 - [7] T. Monz, P. Schindler, J. T. Barreiro, M. Chwalla, D. Nigg, W. A. Coish, M. Harlander, W. Hänsel, M. Hennrich, and R. Blatt Phys. Rev. Lett. 106, 130506 (2011).
 - [8] N. Roy, A. Sharma and R. Mukherjee arXiv:1812.08938
 - [9] K. Kim, M. S. Chang, R. Islam, S. Korenblit, L. M. Duan, and C. Monroe, Phys. Rev. Lett. 103, 120502 (2009).
 - [10] J. W. Britton, B. C. Sawyer, A. C. Keith, C. C. J. Wang, J. K. Freericks, H. Uys, M. J. Biercuk, and J. J. Bollinger, Nature 484, 489 (2012).
 - [11] R. Islam, C. Senko, W. C. Campbell, S. Korenblit, J. Smith, A. Lee, E. E. Edwards, C. C. J. Wang, J. K. Freericks, and C. Monroe, Science 340, 583 (2013).
 - [12] S. Schmid, A. Häter and J. H. Denschlag, Phys. Rev. Lett. 105, 133202 (2010).
 - [13] W. G. Rellergert, S. T. Sullivan, S. Kotochigova, A. Petrov, K. Chen, S. J. Schowalter, and E. R. Hudson Phys. Rev. Lett. 107, 243201 (2011).
 - [14] J. Goold, H. Doerk, Z. Idziaszek, T. Calarco, and Th. Busch Phys. Rev. A 81, 041601(R) (2010).
 - [15] A. Häter and J.H. Denschlag, Contemp. Phys. 55 33 (2014).
 - [16] T. Secker, R. Gerritsma, A. W. Glaetzle, and A. Negretti Phys. Rev. A 94, 013420 (2016).
 - [17] A. Kriukow, A. Mohammadi, A. Härter, J. H. Denschlag, J. Prez-Ros, and C. H. Greene, Phys. Rev. Lett. 116, 193201 (2016).
 - [18] R.M. Kalas and D. Blume, Phys. Rev. A 73, 043608 (2006).
 - [19] F.M. Cucchietti and E. Timmermans, Phys. Rev. Lett. 96, 210401 (2006).
 - [20] W. Casteels, J. Tempere, and J. T. Devreese Phys. Rev. A 83, 033631 (2011).
 - [21] A. T. Grier, M. Cetina, F. Orucevic, V. Vuletic Phys. Rev. Lett. 102, 223201 (2009).
 - [22] L. Ratschbacher, C. Zipkes, C. Sias, and M. Köhl Nat Phys 8, 649 (2012).
 - [23] Z. Idziaszek et. al. Phys. Rev. A 79, 010702 (2009).
 - [24] U. Bissbort, D. Cocks, A. Negretti, Z. Idziaszek, T. Calarco, F. Schmidt-Kaler, W. Hofstetter and R. Gerritsma Phys. Rev. Lett. 111 080501 (2013).
 - [25] J. M. Schurer, P. Schmelcher, and A. Negretti, Phys. Rev. A 90, 033601 (2014).
 - [26] J. M. Schurer, A. Negretti, and P. Schmelcher, New J. Phys. 17, 083024 (2015).
 - [27] J. M. Schurer, R. Gerritsma, P. Schmelcher, and A. Negretti, Phys. Rev. A 93, 063602 (2016).
 - [28] H. Doerk, Z. Idziaszek, and T. Calarco Phys. Rev. A 81, 012708 (2010).
 - [29] R. Gerritsma, A. Negretti, H. Doerk, Z. Idziaszek, T. Calarco, and F. Schmidt-Kaler Phys. Rev. Lett. 109, 080402 (2012).
 - [30] T. Calarco, U. Dorner, P. S. Julienne, C. J. Williams, and P. Zoller Phys. Rev. A 70, 012306 (2004).
 - [31] R. Cote, V. Kharchenko, M. D. Lukin Phys. Rev. Lett. 89, 093001 (2002).
 - [32] J.M. Schurer, A. Negretti, and P. Schmelcher, Phys. Rev. Lett. 119, 063001 (2017).
 - [33] B. Zygelman, Z. Lucic, and E. R. Hudson J. Phys. B: At. Mol. Opt. Phys. 47, 015301 (2014).
 - [34] R. Cote Phys. Rev. Lett. 89, 5316 (2000).
 - [35] K. Ravi, S. Lee, A. Sharma, G. Werth and S.A. Rangwala, Nat. Comm. 3, 1126 (2012).
 - [36] S. Dutta and S. A. Rangwala, Phys. Rev. A 97, 041401(R) (2018).
 - [37] T. F. Gallagher Rep. Prog. Phys. 51 143 (1988).
 - [38] I. Lesanovsky, M. Müller, and P. Zoller Phys. Rev. A 79, 010701(R) (2009).
 - [39] R. Mukherjee, J. Millen, , R. Nath, M. P. A. Jones and T. Pohl J. Phys. B 44, 184010 (2011).
 - [40] R. Grimm, M. Weidemüller, Y. Ovchinnikov Adv. in At. Mol. and Opt. Phys. 42, 95 (2000).
 - [41] C.H. Greene, M. Aymar Phys. Rev. A 44, 1773 (1991).
 - [42] C Dai and X Zhao J. Quant. Spectrosc. Radiat. Transfer 54, 1019 8 (1995).
 - [43] H. Lischka, P. G. Szalay, D. R. Yarkony and R. Shepard Journal of Chem. Phys. 120, 7322 (2004).
 - [44] M. Christandl, N Datta, Artur Ekert and A J Landahl Phys. Rev. Lett. 92, 187902 (2004).
 - [45] T. F. Gallagher. Rydberg Atoms. Cambridge University Press, Cambridge, 1994.
 - [46] J. Millen, G. Lochead and M. P. A. Jones, Phys. Rev. Lett. 105, 213004 (2010).
 - [47] P. McQuillen, X. Zhang, T. Strickler, F. B. Dunning, and T. C. Killian, Phys. Rev. A 87, 013407 (2013).
 - [48] G. Lochead, D. Boddy, D. P. Sadler, C. S. Adams, and M. P. A. Jones, Phys. Rev. A 87, 053409 (2013).
 - [49] L. I. R. Gil, R. Mukherjee, E. M. Bridge, M. P. A. Jones and T. Pohl, Phys. Rev. Lett. 112, 103601 (2014).

- [50] R. Mukherjee, T. C. Killian, and K. R. A. Hazzard, Phys. Rev. A 94, 053422 (2016).
- [51] A.D. Bounds, N.C. Jackson, R.K. Hanley, R. Faoro, E.M. Bridge, P. Huillery, and M.P.A. Jones, Phys. Rev. Lett. 120, 183401 (2018)
- [52] M.A. Norcia, A.W. Young, and A.M. Kaufman Phys. Rev. X 8, 041054 (2018).
- [53] A. Cooper, J. P. Covey, I. S. Madjarov, S. G. Porsev, M. S. Safronova and M. Endres, Phys. Rev. X 8, 041055 (2018).
- [54] L. Couturier, I. Nosske, F. Hu, C. Tan, C. Qiao, Y. H. Jiang, P. Chen, M. Weidemüller, arXiv:1810.07611
- [55] F. Hu, I. Nosske, L. Couturier, C. Tan, C. Qiao, P. Chen, Y. H. Jiang, M. Weidemüller, arXiv:1812.01258
- [56] J. Deiglmayr, A. Göritz, T. Best, M. Weidemüller, and R. Wester, Phys. Rev. A 86, 043438 (2012).
- [57] S. Wüster, C. Ates, A. Eisfeld, and J. M. Rost, New J. Phys. 13, 73044 (2011).